CHAPTER V

POLYLACTIDE COMPOUNDING FOR INJECTION MOLDING PRODUCT

5.1 ABSTRACT

This research has an aim to improve the thermal and mechanical properties of polylactide (PLA) by copolymerization between a lactide monomer and epoxidized natural rubber (ENR) using stannous (II) octoate ($Sn(Oct)_2$) as an catalyst. In a twin-screw extruder, ENR-g-PLA copolymer was prepared using 0.1 to 0.3 wt% of catalyst and 70/10/20 to 85/10/5 wt% of PLA/LA/ENR respectively. The ENR-g-PLA copolymer was successfully synthesized and confirmed by FT-IR spectra. The occurrence peak at 1740 cm^{-1} and 3400 cm^{-1} corresponded to the carbonyl group (C=O) and hydroxyl group (-OH) which resulted from the reaction between PLA and ENR. The calculation of grafting showed that there was 24%grafting of ENR on PLA. Also, the degree of grafting was directly proportional to various ENR contents. In the comparison between neat PLA and ENR-g-PLA copolymer, DSC thermograms suggested that T_g reduced to 44.8 °C from 57 °C (neat PLA). The result of mechanical property measurement according to ASTM-D826, revealed that the impact strength increased in the presence of ENR. The impact strength of ENR-g-PLA increased 1.5-folds in comparison to pure PLA. The elongation of copolymer was measured by universal testing machine, showing the elongation was improved compared to pure PLA. Moreover, the morphology of copolymer was studied by FE-SEM. The results revealed the well dispersion phase of ENR in PLA matrix.

Keywords: Epoxidized natural rubber, Lactide monomer, Polylactide, Ring-opening polymerization, Stannous (II) octoate.

5.2 INTRODUCTION

The use of stationary produces from plastic in our daily cause the plastic waste problems. The information from Pollution Control Department was reported that the amount of plastic waste is 2.7×10^6 tons/year (Pollution Control Department, 2008). The growing of plastic waste is the most serious problem for environmental and life quality that can recognize and solve urgently. Therefore, biodegradable plastics can be replaced the commodity plastics for reducing the large amount of plastic waste problem. The biodegradable polymers can be classified by two categories: (1) renewable resources, such as polyhydroxyalkanoate (PHA), polylactide (PLA), thermoplastics starch (TPS), cellulose and protein. ; (2) petrochemical resources, such as, aliphatic polyester and copolyester, aromatic polyester and copolyester, poly(caprolactone) (PCL), poly(esteramide)s (PEA) and poly(vinyl alcohol) (PVA) [1].

Polylactide (PLA) is hydrophobic aliphatic polyester that the mechanical and thermal properties are comparable with the traditional thermoplastics. PLA is prepared by two ways, the polycondensation polymerization of lactic acid and the ring-opening polymerization of lactide. The ring-opening polymerization of lactide is the way to get high molecular weight of PLA. Not only the polymerization method, but the temperature of mixing and the catalyst content also affect to molecular weight. Hyon *et al.* synthesized polylactide with different molecular weight. They found that the increase of temperature and catalyst content resulted in the decrease in molecular weight [2]. Moreover, PLA is being commercially produced for commodity application [3]. For example, fibers were produced from PLA exhibit low odor retention and excellent moisture absorption properties [4], the internal fixation of bone fractures were produced from PLA for medical application [5], and PLA can be formed by injection molding as several objects. Even through, PLA has many advantage properties but it has some disadvantages such as, rigidity, slow rate of crystallization and heat deflection temperature [6].

There are several methods to overcome the limitation of PLA such as processing, plasticization, blending, and copolymerization. The great method to improve limitation of PLA is copolymerization of lactide or lactic acid monomer with the other monomers because it is not occurred phase separation. There are two ways to prepare copolymer of PLA. The first way is polycondensation of lactic acid copolymerized with other monomers that produced low molecular weight copolymer. The second way is ring-opening copolymerization of lactide monomer with cyclic monomer that produced high molecular weight copolymer. Nooeaid *et al.* successfully synthesized the EVOH-g-PLA copolymer in Barbender mixer. The composition of EVOH/LA at 50/50 wt% gave the highest molecular weight (Mw = 36.6 x 10^4 g/mol) and the amount of graft copolymer. Furthermore, the optimum of mechanical properties was found in this composition [7].

Epoxidized Natural Rubber (ENR) is the natural rubber that some part of double bonds is replaced by epoxide groups. ENR has many good mechanical and thermal properties offering high strength, due to their ability to undergo strain crystallization, along with increase glass transition temperature and high degree of damping [7]. There are many researchers studied ENR blend with other polymers to improve properties of each polymer. For example, Charoen Nakason *et al.* blended ENR with poly(methyl methacrylate) to improve the mechanical, thermal and morphological properties [8]. Moreover, G.H. Yew *et al.* blended ENR with poly(lactic acid)/rice starch to improve brittleness of poly(lactic acid), the result showed that poly (lactic acid) had more rubbery behavior [9].

The purpose of this research is to improve the toughness of PLA by copolymerization between lactide monomer and epoxidized natural rubber using stannous (II) octoate ($Sn(Oct)_2$) as an catalyst. The epoxy group in ENR can initiate the ring-opening polymerization of lactide monomer. This leads to high molecular weight and toughness improvement of PLA. There by, this work studies the effect of the blend ratio and the catalyst concentration on the morphology, mechanical properties, thermal properties and biodegradability of PLA/ENR copolymer.

5.3 EXPERIMENTAL

5.3.1 Materials

L-lactide monomer ((3*S*)-*cis*-3,6-Dimethyl-1,4-dioxane-2,5-dione), (CAS No. 4511-42-6) (99.5% purity) was purchased from Shenzhen Brightchina Industrial Co.,Ltd. Polylactide (3052D) (CAS No. 33135-50-1) was purchased from BC Polymer Co., Ltd. Epoxidized Natural Rubber (ENR) (25% epoxy group) (CAS No. 138009-59-3) was purchased from PARATHAI. Stannous (II) Octoate ($Sn(Oct)_2$)) as a catalyst (CAS No. 301-10-0) was purchased from Sigma aldrich.

Chloroform ($CHCl_3$) (CAS No. 67-66-3) and toluene ($C_6H_5CH_3$) (CAS No. 108-88-3) were purchased from Lab Scan Co.,Ltd.

5.3.2 Preparation of LA/ENR in Brabender mixer

In Brabender mixer, the amount of the blending between lactide monomer (10 wt%) and epoxidized natural rubber (5, 10, 15, 20 wt%) mixed with various catalyst concentration (1, 2, 3 wt%) as shown in Table 5.1. First, epoxidized natural rubber 20 g and stannous (II) octoate were added to the chamber for 5 minute. Then, lactide monomer 40 g was added and further mixed for 30 minute. The temperature of mixing was 160 °C and rotor speed was maintained at 20 rpm. The whole mass of LA/ENR was carried out for further process.

Table 5.1 The mixtures of LA/ENR in Brabender mixer

Ingredient	**Quantity (wt%)**			
ENR	5	10	15	20
Lactide monomer	10	10	10	10
Catalyst	0.1, 0.2, and 0.3	0.1, 0.2, and 0.3	0.1, 0.2, and 0.3	0.1, 0.2, and 0.3

5.3.3 Preparation of ENR-g-PLA in twin-screw extruder

In twin-screw extruder, the whole mass of LA/ENR copolymer (10/20, 10/15, 10/10, and 10/5 wt% of LA/ENR) from Brabender mixer was carried out and continuously blended with pure PLA by varying the amount of PLA/LA/ENR between 70/10/20, 75/10/15, 80/10/10, and 85/10/5 wt% and varying the amount of stannous (II) octoate between 0.1 and 0.3 wt%. The processing condition is shown in Table 5.2 and the mixtures are indicated in Table 5.3. The mechanical and thermal properties of copolymer were measured.

Table 5.2 Processing condition of PLA/LA/ENR copolymerization

Type	Temperature (°C)										Speed screw (rpm)
	Z1	Z2	Z3	Z4	Z5	Z6	Z7	Z8	Z9	Die	
PLA/LA/ENR copolymerization (0.1, 0.2, and 0.3 wt% $Sn(Oct)_2$)	150	155	160	160	160	160	165	165	165	170	30

Table 5.3 The mixtures of PLA/LA/ENR copolymerization in twin-screw extruder

Ingredient	Quantity(wt%)			
Polylactide	70	75	80	85
L-lactide monomer	10	10	10	10
ENR	20	15	10	5
Catalyst	0.1, 0.2 and 0.3	0.1, 0.2 and 0.3	0.1, 0.2 and 0.3	0.1, 0.2 and 0.3

5.3.3 Characterizations

. The functional group of ENR-g-PLA copolymer was analyzed by Thermo Nicolet Nexus 670 FTIR spectrometer. The specimens were prepared by compression molding into film. The spectra were recorded over the wave number range of 4000 - 400 cm^{-1} with 32 scans at a resolution of 4 cm^{-1}.

The grafting percentage of copolymer was determined by Soxhlet extractor (VELP SCIENTIFICA, SER 148) with paper thimble. Chloroform and toluene were used to extract the copolymer at 180 °C for 3 hours. After that, the resulting yields were dried in vacuum oven at 80 °C. The grafting percentage was calculated as shown in Eq.5.1 [10].

$$Grafting\ percentage = \frac{W_{graft\ copolymer}(g) - W_{PLA}(g)}{W_{PLA}(g)} \times 100\% \quad (Eq.5.1)$$

Thermal stability of copolymer was determined by Perkin-Elmer Pyris Daimond thermogravimatric analysis (maximum temperature is 1,000 °C). The weight of sample was in the range of 5-10 mg. and was heated at the heating rate of 10 °C/min from 30-800 °C in nitrogen atmosphere.

Thermal properties analyses were carried out by using Metller Toledo, DSC 822. The weight of sample will be in the range of 4-10 mg. The samples were first heated from 30 °C to 200 °C and cooled down with a flow rate of 10 ml/min to -60 °C. The samples were then reheated to 200°C at the same rate.

The dynamic mechanical property of copolymer was carried out by using a dynamic-mechanical analyzer GABO EPLEXOR QC 25 instrument. The samples were 13 mm x 55 mm x 3 mm (width x length x thickness). The testing temperature was set from -80 to 120 °C, 10 Hz for frequency. Static and dynamic strains were 10% and 5%, respectively. The tension mode was used.

The impact strengths were identified by Izod impact testing according to ASTM-D826 using the ZWICK 5113 Pendulum Impact Tester with the pendulum load of 21.6 J. The average values of five samples were reported.

The tensile properties were tested by using an Instron 4206 universal testing machine with cross-head speed of 50 mm/min. The samples were in the dumbbell-shape. The size of sample specimen was 13 mm width of narrow section, 90 mm length of narrow section, and 3 mm thickness.

The morphology of copolymer was carried out by using FE-SEM that was performed on Hitachi, S-4800 Model. The extrudates obtained from twin-screw extruder were broken in liquid nitrogen. Then, the samples were etched by toluene around 10 minute and dried in vacuum oven at 80 °C overnight. After that, all of specimens were coated with platinum under vacuum.

The copolymers were tested according to ASTM D5988 - 03 (Standard Test Method for Determining Aerobic Biodegradation in Soil of Plastic Materials or Residual Plastic Materials after Composting).

The melt flow index of copolymer was measured by using Zwick, Model 4105 melt flow indexer. The weight of sample was in range of 5-8 g. The temperature processing was 150 °C. The melt was driven through a capillary die using a 1 kg piston, melting time 120 seconds, and cutting time 30 seconds. The average values of five samples were reported.

5.4 RESULTS AND DISCUSSION

5.4.1 Chemical analysis

The functional groups of the copolymer are confirmed by Fourier transform infrared spectroscopy (FT-IR). FT-IR spectra of neat-PLA, ENR and ENR-g-PLA synthesized with various catalyst concentrations are shown in Figure 5.

1 and 5.2.The characteristic peaks of PLA are observed at 1740 cm^{-1} attributed to carbonyl (C=O stretching) in chain of PLA [7]. At 894 and 1655 cm^{-1} are assigned to =CH-bending and =CH-stretching which are one of the functional groups of ENR. The FT-IR spectra of copolymer have the same peak of PLA and ENR. Furthermore, there two transmission peaks at 1190 cm^{-1} and 1090 cm^{-1} reveal the symmetric C-O-C stretching of the ester group. The two other peaks at 1130 cm^{-1} and 1370 cm^{-1}, attributed to C-CH_3 stretching and C-H bending in CH_3 group. Moreover, there are two other peaks at 1130 cm^{-1} and 1370 cm^{-1}, attributed to C-CH_3 stretching and C-H bending in CH_3 group. In addition, the peak around 3400 cm^{-1} shows the presence of the reactive functional group (-OH) used as the reactive sites for graft copolymerization of ENR to PLA [8].

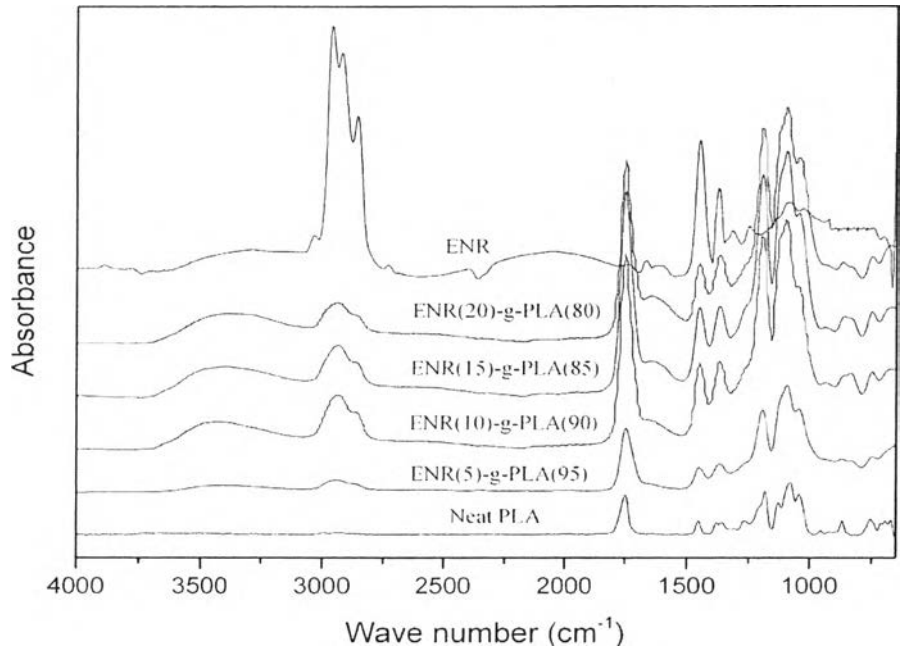

Figure 5.1. FT-IR pattern of neat PLA, ENR, and ENR-g-PLA with various ENR contents.

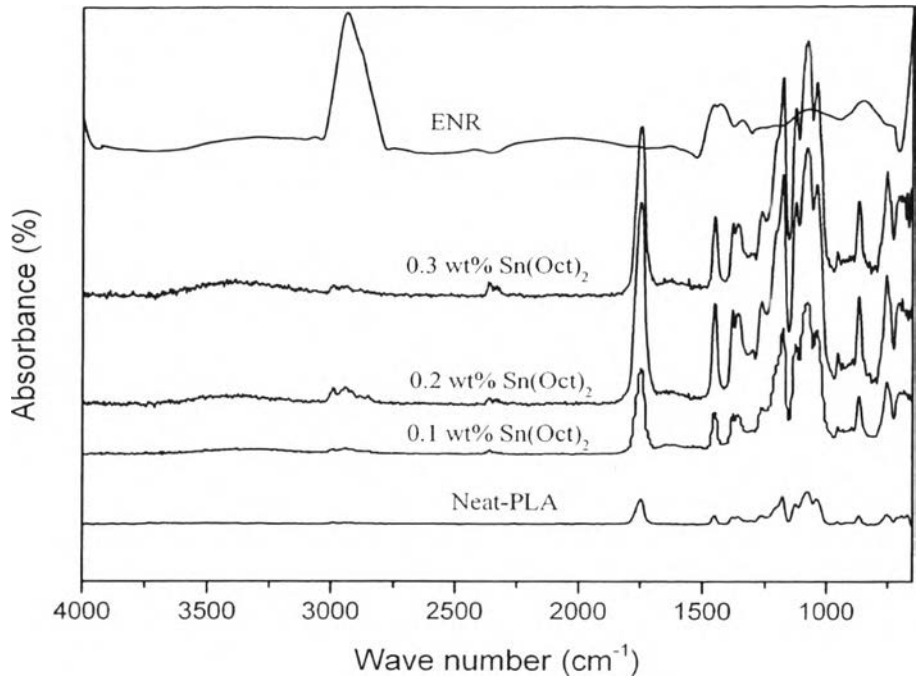

Figure 5.2. FT-IR pattern of neat PLA, ENR, and ENR-g-PLA with various catalyst concentrations.

5.4.2 The grafting percentage of ENR on PLA main-chain.

The copolymer between ENR and PLA (ENR-g-PLA) is extracted by toluene and chloroform in Soxhlet extractor. The grafting percentage of ENR on PLA at different ENR contents and catalyst concentrations are presented in Figure 5.3. The grafting percentage values are shown in Table 5.3. The %grafting of ENR on PLA increases from 1% to 24% as the ENR content increase from 5 wt% to 20 wt%. This result demonstrates that the increasing of ENR content results in the increase reaction between PLA and ENR [10]. Moreover, the increasing of catalyst causes the high generated copolymer. The maximum %grafting is obtained at 0.2 wt% of a catalyst concentration. After the amount of catalyst over 0.2 wt%, the chain scission is occurred leading to the decreasing of the %grafting [3].

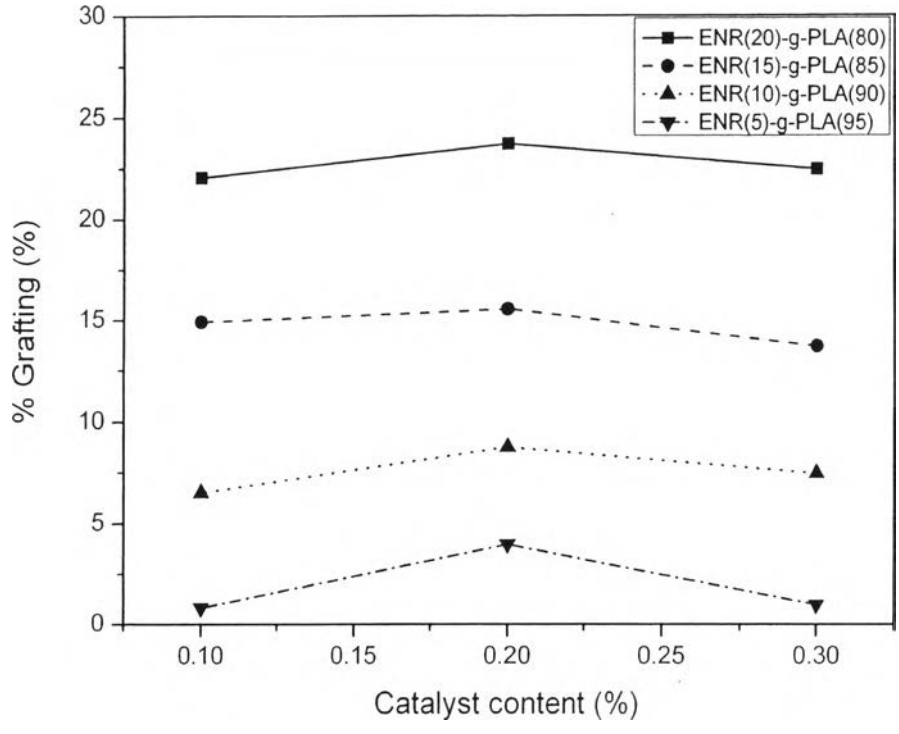

Figure 5.3. The grafting percentage of ENR on PLA at various ENR and catalyst contents.

Table 5.4 The grafting percentage values of copolymer

Sample (wt %)	Catalyst concentration (wt %)	% grafting
ENR(5)-g-PLA(95)	0.10	22.1
	0.20	23.7
	0.30	22.4
ENR(10)-g-PLA(90)	0.10	14.9
	0.20	15.5
	0.30	13.7
ENR(15)-g-PLA(85)	0.10	6.5
	0.20	8.8
	0.30	7.4
ENR(20)-g-PLA(80)	0.10	0.8
	0.20	4.0
	0.30	1.0

5.4.3 Thermal stability of copolymer

The thermal stability of neat PLA, pure ENR and ENR-g-PLA copolymer is shown in Figure 5.4 to 5.8. The graph shows one-stage weight loss of each sample. The decomposition temperature decreases with the presence of ENR from 355.3 to 332.8 °C in the Table 5.4 due to the higher flexibility at double bonds in the ENR chain causing the easier movement of the copolymer molecule at elevated temperature [11].

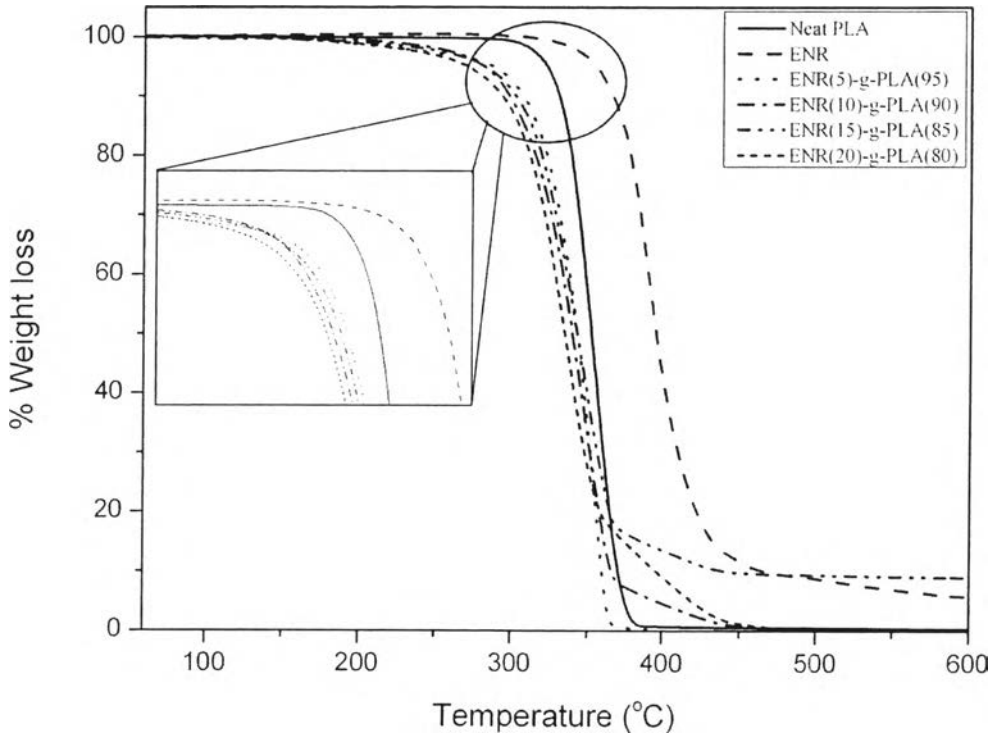

Figure 5.4. TGA curve of neat PLA, ENR pure and ENR-g-PLA at 0.1 wt% $Sn(Oct)_2$ with various ENR content.

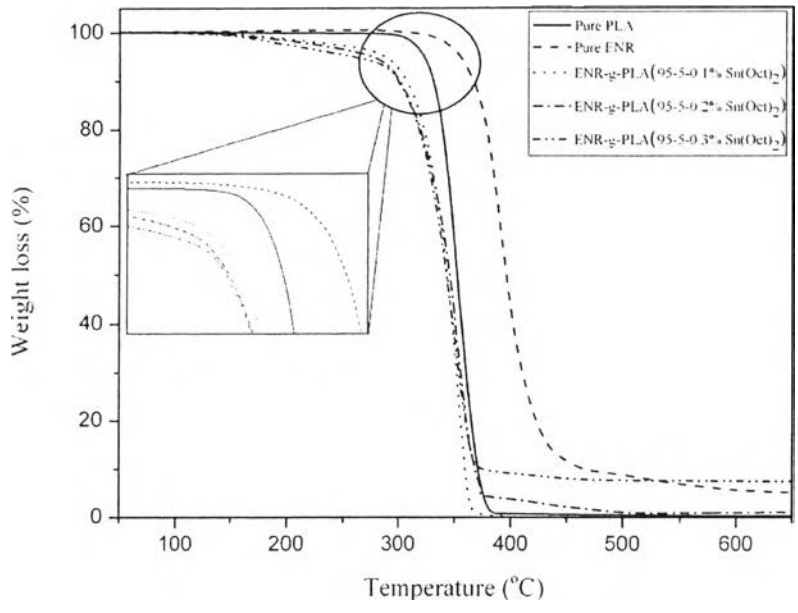

Figure 5.5. TGA curve of neat PLA, ENR pure and ENR-g-PLA at 95/5 wt% PLA/ENR content with various catalyst concentration.

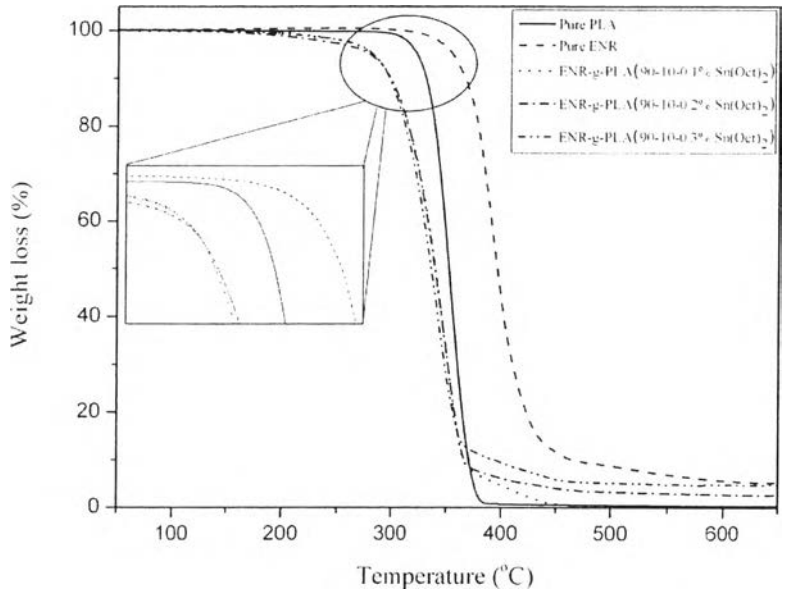

Figure 5.6. TGA curve of neat PLA, ENR pure and ENR-g-PLA at 90/10 wt% PLA/ENR content with various catalyst concentration.

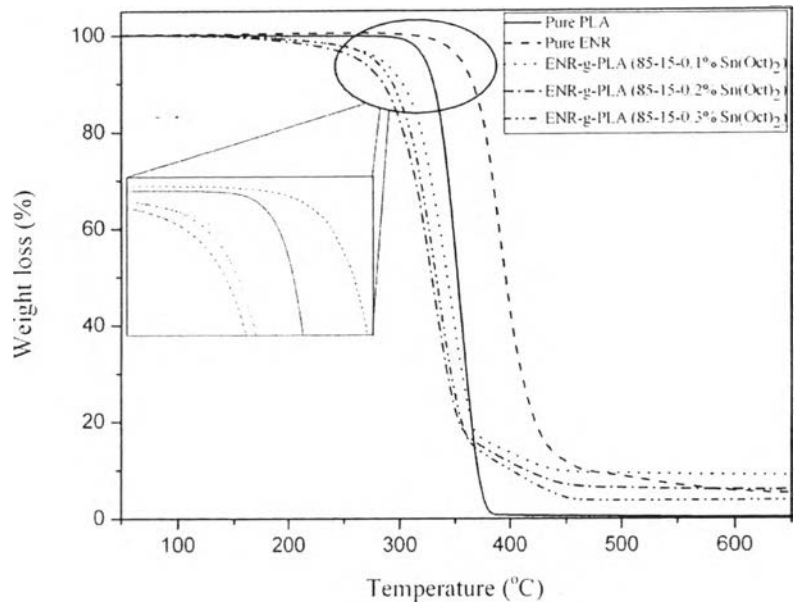

Figure 5.7. TGA curve of neat PLA, ENR pure and ENR-g-PLA at 85/15 wt% PLA/ENR content with various catalyst concentration.

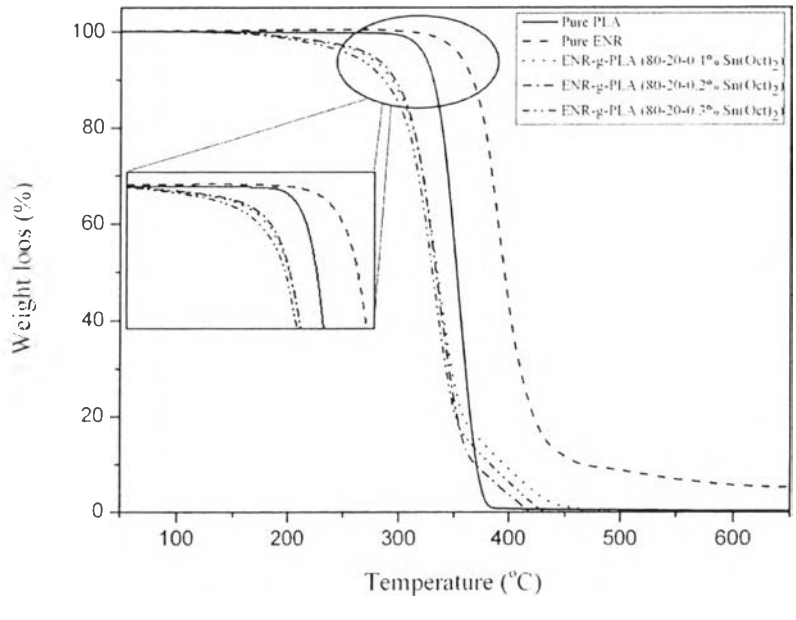

Figure 5.8. TGA curve of neat PLA, ENR pure and ENR-g-PLA at 80/20 wt% PLA/ENR content with various catalyst concentration.

Table 5.5 The decomposition temperatures of copolymers

Composition of PLA-LA-ENR (wt%)	**Catalyst content (wt%)**	**Decomposition Temperature (^{o}C)**
Pure PLA	-	332.8
Pure ENR	-	390.8
85-10-5	0.1	355.3
	0.2	354.4
	0.3	350.0
80-10-10	0.1	346.8
	0.2	345.4
	0.3	338.4
75-10-15	0.1	346.6
	0.2	334.6
	0.3	331.3
70-10-20	0.1	336.6
	0.2	334.1
	0.3	332.5

5.4.4 Thermal properties of copolymer

The thermal properties of pure PLA and copolymer were characterized by using DSC measurement. The DSC thermograms of pure PLA and copolymer are shown in Figure 5.9 to 5.10. The values of thermal properties are shown in the Table 5.5. There are two glass transition temperatures (T_{g1} and T_{g2}). The T_{g1} corresponds to ENR which has no shift in ENR-g-PLA. The T_{g2}, T_{cc} and T_m tend to decrease resulting from higher content of ENR in the materials. The increasing the amount of ENR can reduce the crystallization induction causing the lower crystallinity of PLA. [12]. There are two melting transitions of melting temperature which occur at around 136 and 146 °C corresponding to the PLA crystal induced by ENR and the more perfect crystalline form of PLA respectively [13]. Furthermore, the higher catalyst concentration increases the %crystallinity because of the chain scission effect [14].

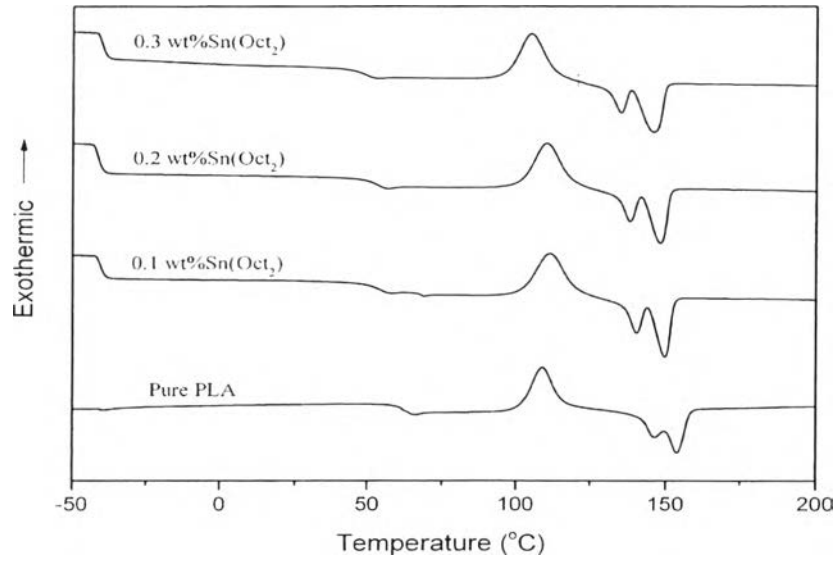

Figure 5.9. DSC thermograms of neat PLA and ENR-g-PLA at 95/5 wt% PLA/ENR content with various catalyst concentrations.

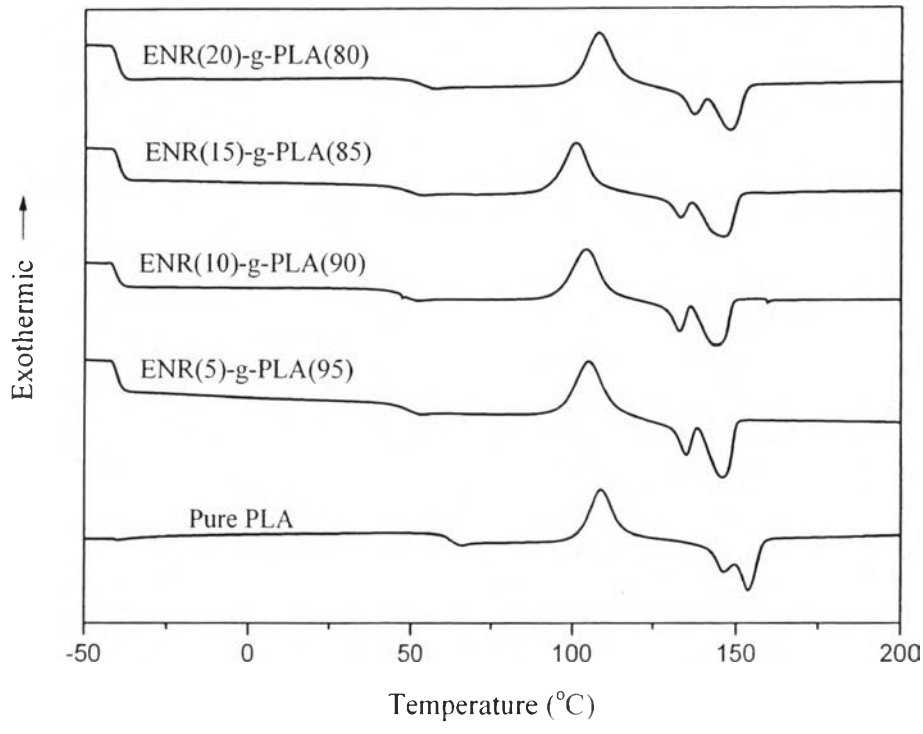

Figure 5.10. DSC thermograms of neat PLA and ENR-g-PLA at 95/5 wt% PLA/ENR content with various ENR content.

Table 5.6 The thermal property of neat PLA and ENR-g-PLA

Catalyst concentration	Sample	T_{g1} (°C)	T_{g2} (°C)	T_{cc} (°C)	T_{m1} (°C)	T_{m2} (°C)	ΔH_{cc} (J/g)	ΔH_m (J/g)	$\%X_c$ *
-	Pure PLA	-	59.8	103.0	146.8	153.7	19.4	24.5	5.4
0.1 wt%	ENR(5)-g-PLA(95)	-41.9	49.3	111.4	139.8	149.7	31.8	34.1	2.5
	ENR(10)-g-PLA(90)	-41.2	47.1	109.2	136.7	147.0	29.9	32.1	2.4
	ENR(15)-g-PLA(85)	-40.2	45.0	107.7	136.5	146.0	29.3	30.3	1.2
	ENR(20)-g-PLA(80)	-40.0	44.9	105.7	136.4	146.1	27.5	28.2	0.8
0.2 wt%	ENR(5)-g-PLA(95)	-41.5	48.0	110.8	137.3	148.6	32.4	35.6	3.6
	ENR(10)-g-PLA(90)	-41.8	45.1	107.0	136.7	143.7	29.3	31.6	2.5
	ENR(15)-g-PLA(85)	-40.2	44.8	106.6	136.5	148.2	27.8	29.1	1.4
	ENR(20)-g-PLA(80)	-40.2	43.9	108.0	136.4	148.0	30.2	30.9	0.9
0.3 wt%	ENR(5)-g-PLA(95)	-41.8	45.3	110.2	135.0	148.1	31.0	35.3	4.9
	ENR(10)-g-PLA(90)	-41.4	44.5	105.9	136.7	148.6	30.8	33.9	3.6
	ENR(15)-g-PLA(85)	-40.3	43.8	105.9	136.5	148.7	29.0	30.3	1.5
	ENR(20)-g-PLA(80)	-40.8	42.8	101.7	136.4	144.0	26.1	27.1	1.0

* $\%X_c = ((\Delta H_m - \Delta H_{cc})/\Delta H_m^0) / \Phi PLA \times 100$

5.4.5 Dynamic mechanical properties

The dynamic mechanical properties are characterized by using a dynamic-mechanical analyzer GABO EPLEXOR QC 25 instrument. The storage modulus and loss modulus of copolymers depend on temperature are shown in Figure 5.11. to 5.14. The figures are indicated that there is a large drop of storage modulus around glass transition temperature of PLA. Moreover, the storage modulus manifests the stiffness of copolymer. At room temperature (~30 °C), the storage modulus of copolymer decreases with the increment of ENR content, owing to the long flexibility chain of ENR which exhibited the rubbery behavior at room temperature resulting in the reduction of crystallinity of copolymer [6]. The loss modulus represents the dissipated energy of copolymer. The loss modulus increases with increasing of ENR contents relating to melt flow index of copolymer (Table 5.8). The higher loss modulus resulting in more dissipate energy of copolymer. Besides, T_g from tan δ shifts to lower temperature with increasing ENR content corresponding to T_g from DSC due to flexible chain movement.

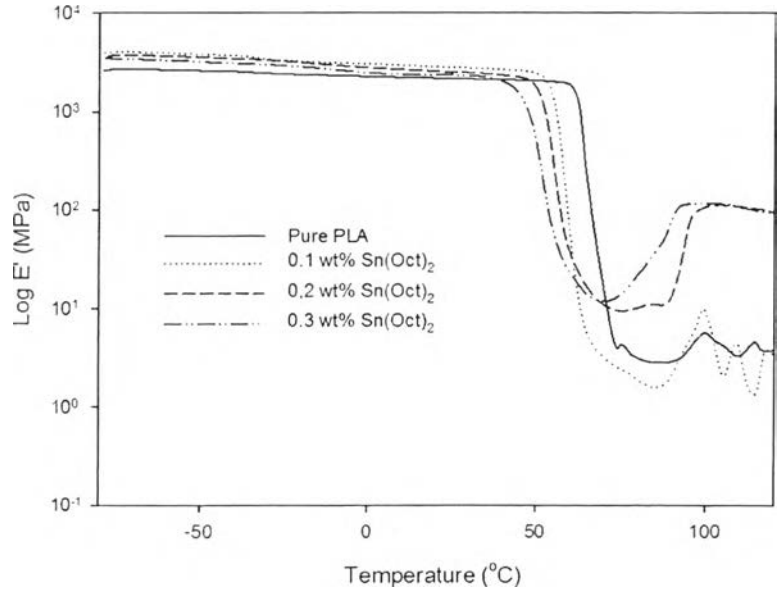

Figure 5.11. The storage modulus of ENR(5)-g-PLA(95) copolymer with different catalyst concentrations.

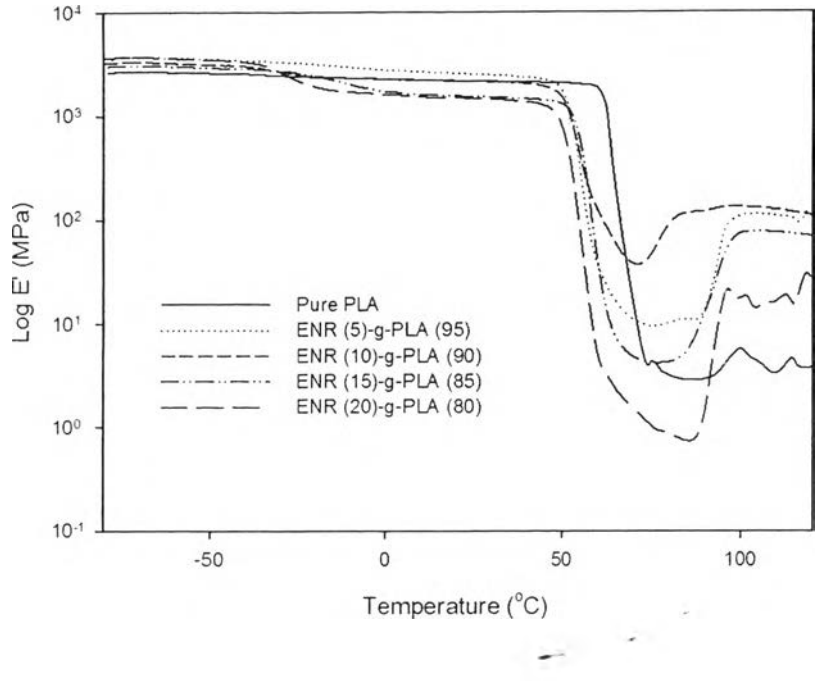

Figure 5.12. The storage modulus of copolymer with different ENR contents at 0.2 wt% of $Sn(Oct)_2$.

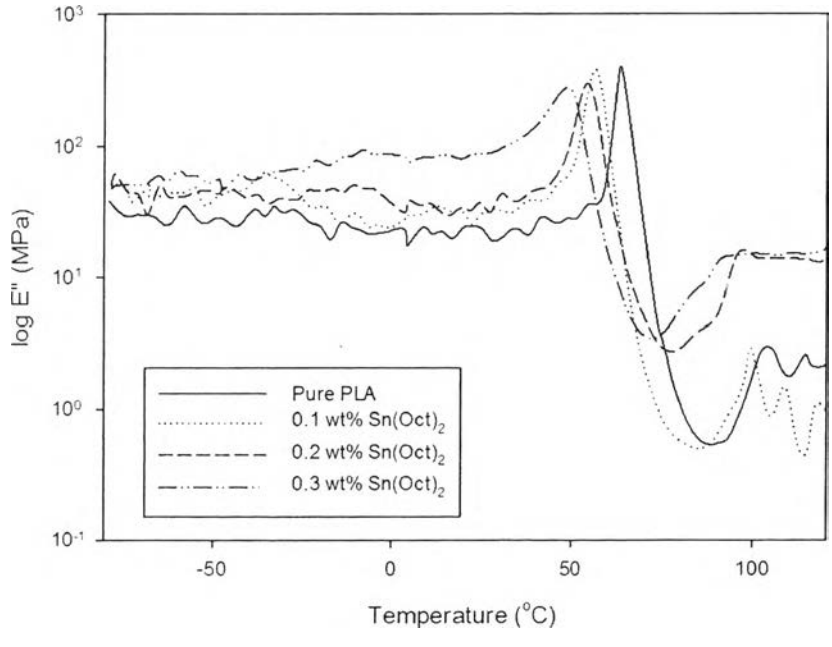

Figure 5.13. The loss modulus of ENR(5)-g-PLA(95) copolymer with different catalyst concentrations.

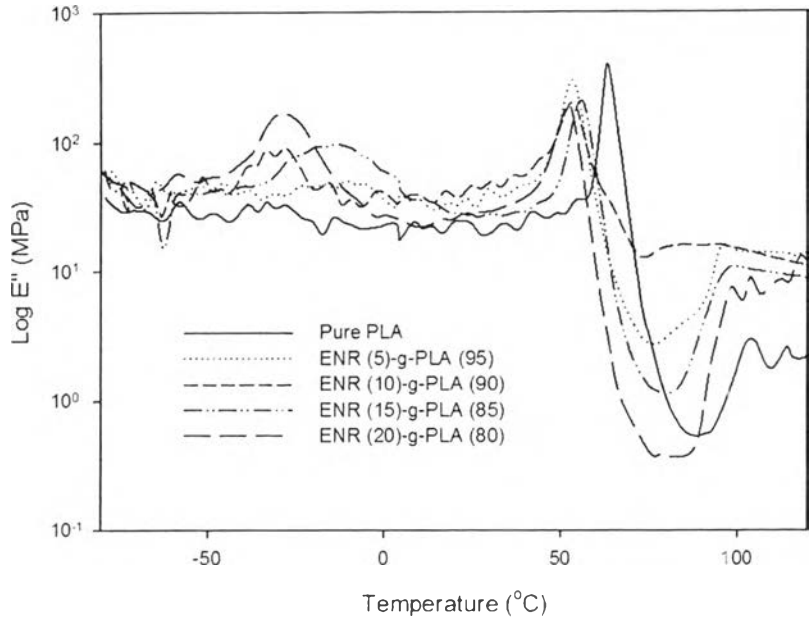

Figure 5.14. The loss modulus of copolymer with different ENR contents at 0.2 wt% of $Sn(Oct)_2$.

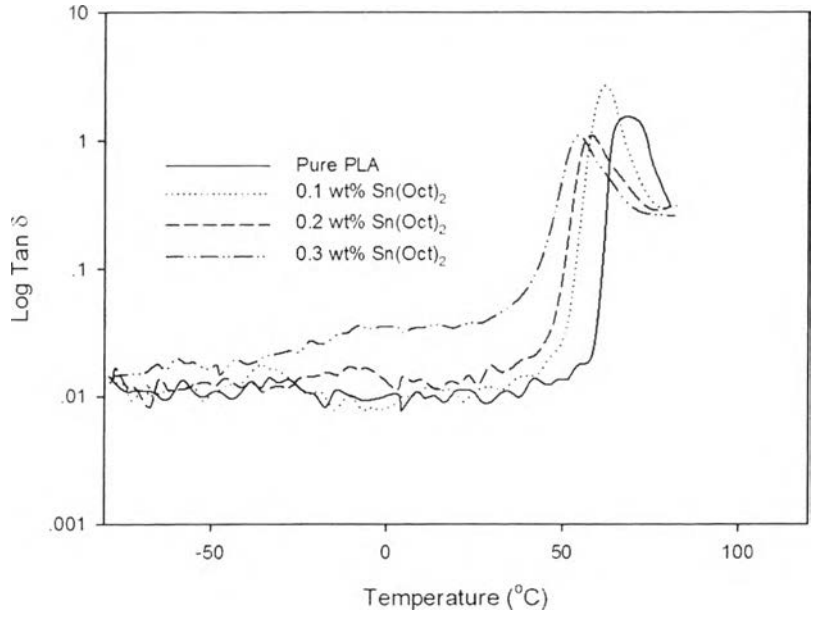

Figure 5.15. Tan δ of ENR(5)-g-PLA(95) copolymer with different catalyst concentrations.

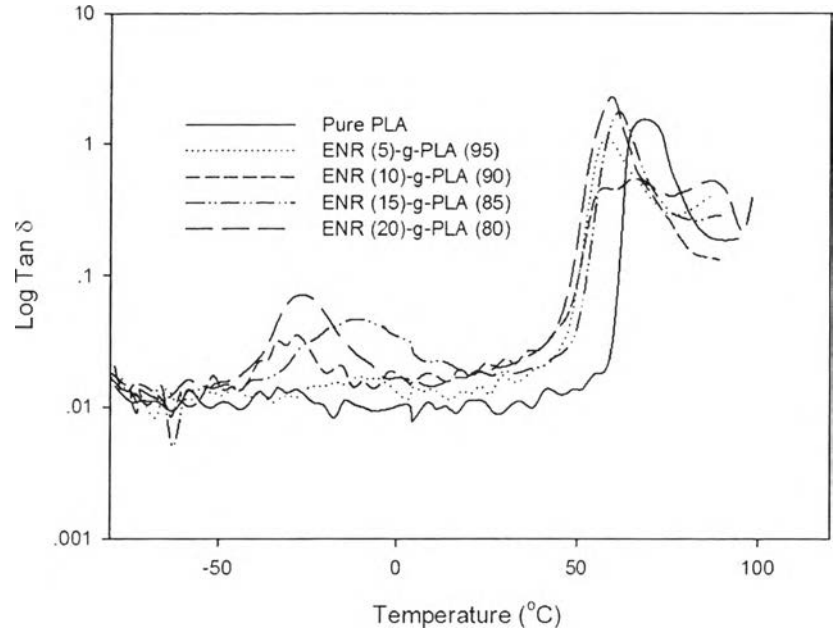

Figure 5.16. Tan δ of copolymer with different ENR contents at 0.2 wt% of $Sn(Oct)_2$.

5.4.6 The impact strength of copolymer

The impact strength of ENR-g-PLA copolymers is illustrated in Table 5.6 and Figure 5.17. Their impact strengths increase from that of the neat PLA because epoxidized natural rubber can dissipate energy by dispersing rubber phase resulting in avoiding an abrupt breaking. However, the impact strength is hardly depending on the amount of ENR and excess ENR turns to poorer impact strength due to the agglomeration of ENR phase was observed. However, the results clearly suggest that the optimum amount of ENR used by this method is 15 wt%. The impact strength is controlled by several factors such as size and shape of the rubber phase, interfacial adhesion between rubber particles and matrix, processing condition and blending methods [15].

Table5.7 The value of impact strength of neat PLA and copolymer

Sample	Impact strength (kJ/m^2)		
	0.1 wt% $Sn(Oct_2)$	0.2 wt% $Sn(Oct_2)$	0.3 wt% $Sn(Oct_2)$
Neat PLA	4.6±0.15	4.6±0.15	4.6±0.15
ENR(5)-g-PLA(95)	6.4±0.20	6.3±0.15	5.8±0.31
ENR(10)-g-PLA(90)	6.6±0.15	6.5±0.10	6.1±0.12
ENR(15)-g-PLA(85)	6.8±0.10	6.7±0.26	6.3±0.31
ENR(20)-g-PLA(80)	6.0±0.06	5.9±0.17	5.5±0.06

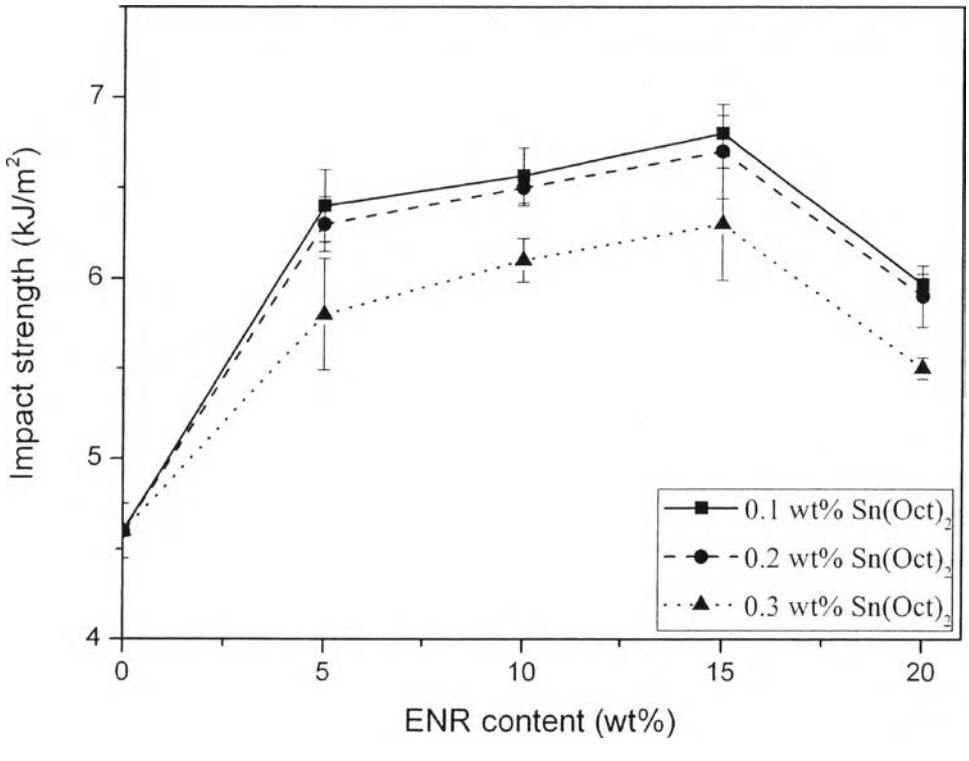

Figure 5.17. The impact strength of copolymer.

5.4.7 Tensile properties

The tensile properties of copolymers are characterized by using an Instron 4206 universal testing machine. The stress-strain curve of copolymer with different ENR content and catalyst concentration are shown in Figure 5.18 and Figure 5.19., respectively. The tensile strength, Young's modulus, and percent elongations at break values are shown in Table 5.7. The tensile strength of copolymer decreases with the ENR content increase. However, the Young's modulus of copolymer decreases with the increment of ENR content that attributed to elastomeric behavior [16]. The elongation at break of copolymer increases with the increasing of ENR content, but over 15 wt% ENR content the elongation at break decreases due to the agglomeration of ENR particle. These results correspond to SEM image of higher ENR content in PLA matrix.

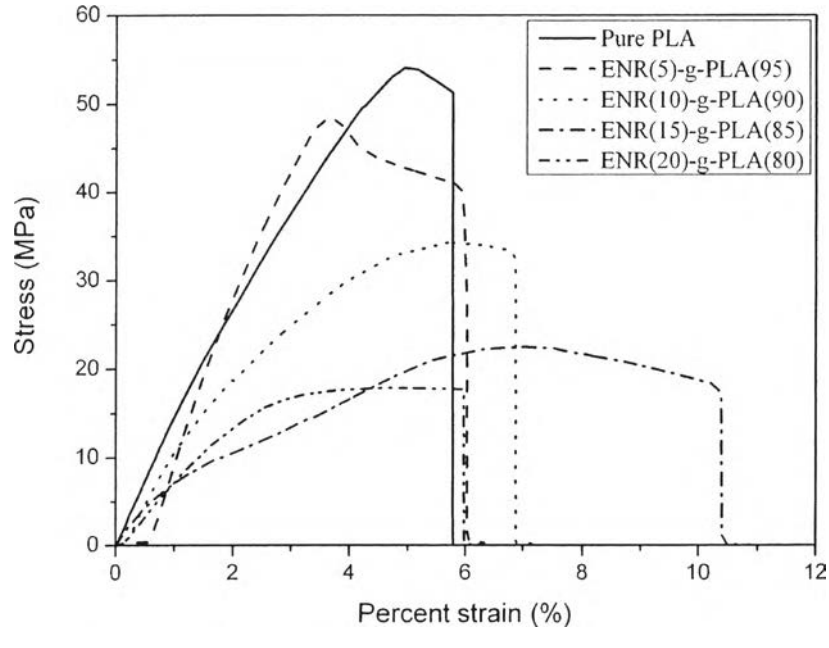

Figure 5.18. The stress-strain curve of copolymer at 0.1 wt% $Sn(Oct)_2$ with different catalyst concentration.

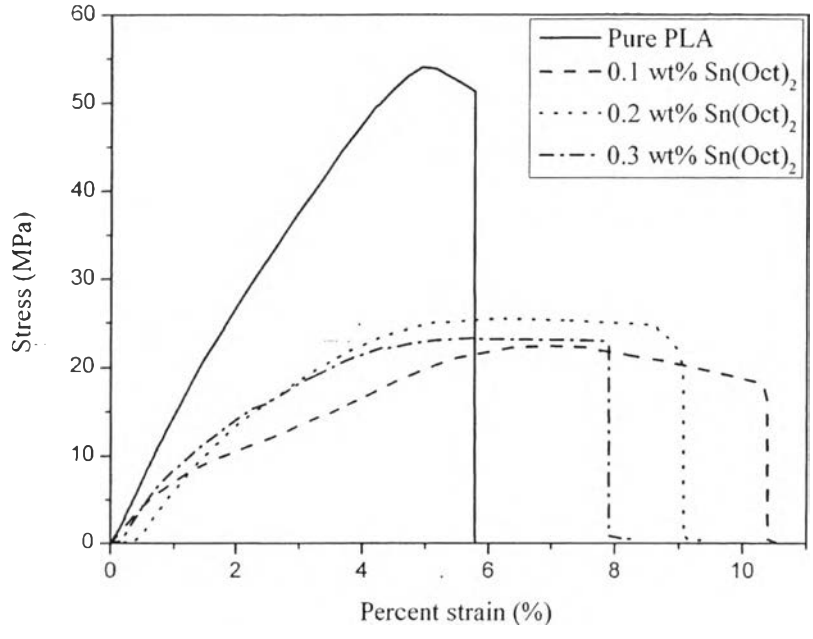

Figure 5.19. The stress-strain curve of copolymer at 85/15 wt% of PLA/ENR content with different catalyst concentration.

Table 5.8 The tensile properties of copolymer

Sample	Catalyst concentration (wt%)	Tensile strength (MPa)	Young' modulus (MPa)	Elongation at Break (%)
Pure PLA	-	51.44 ± 1.3	1556.38 ± 9.5	5.72 ± 0.12
ENR(5)-g-PLA(95)	0.1	39.18 ± 0.45	2237.28 ± 71.6	5.94 ± 0.01
	0.2	39.42 ± 1.5	2014.05 ± 19.2	5.41 ± 0.14
	0.3	39.62 ± 1.8	1989.15 ± 28.3	5.05 ± 0.04
ENR(10)-g-PLA(90)	0.1	32.86 ± 1.7	1440.41 ± 9.9	6.82 ± 0.35
	0.2	33.01 ± 1.8	1488.53 ± 9.10	6.32 ± 0.08
	0.3	35.40 ± 2.1	1421.38 ± 17.58	6.04 ± 0.04
ENR(15)-g-PLA(85)	0.1	21.26 ± 1.9	934.61 ± 16.54	9.25 ± 0.09
	0.2	21.63 ± 0.65	1071.7 ± 9.30	9.02 ± 0.20
	0.3	22.86 ± 2.5	1193.0 ± 10.20	7.90 ± 0.12
ENR(20)-g-PLA(80)	0.1	17.70 ± 0.13	920.70 ± 16.2	5.93 ± 0.32
	0.2	18.36 ± 2.3	941.44 ± 21.7	5.40 ± 0.25
	0.3	16.29 ± 0.9	949.74 ± 10.8	5.01 ± 0.18

5.4.8 The morphology of copolymer

The morphology of copolymers is determined by using FE-SEM-Hitachi, S-4800 Model. The SEM images of copolymer compared with pure PLA are represented in Figure 5.20 and Figure 5.21. The SEM micrograph indicates that the increasing in ENR contents leads to more dispersed phase existed in PLA matrix. However, the enhancement in the amount of ENR decreases the dispersion in PLA phase due to the agglomeration of ENR which is observed from the large porosity with the size of 4 - 12 μm. Furthermore, the addition of catalyst resulted in polymerization between PLA and ENR, does not effects to the dispersion of ENR in PLA matrix.

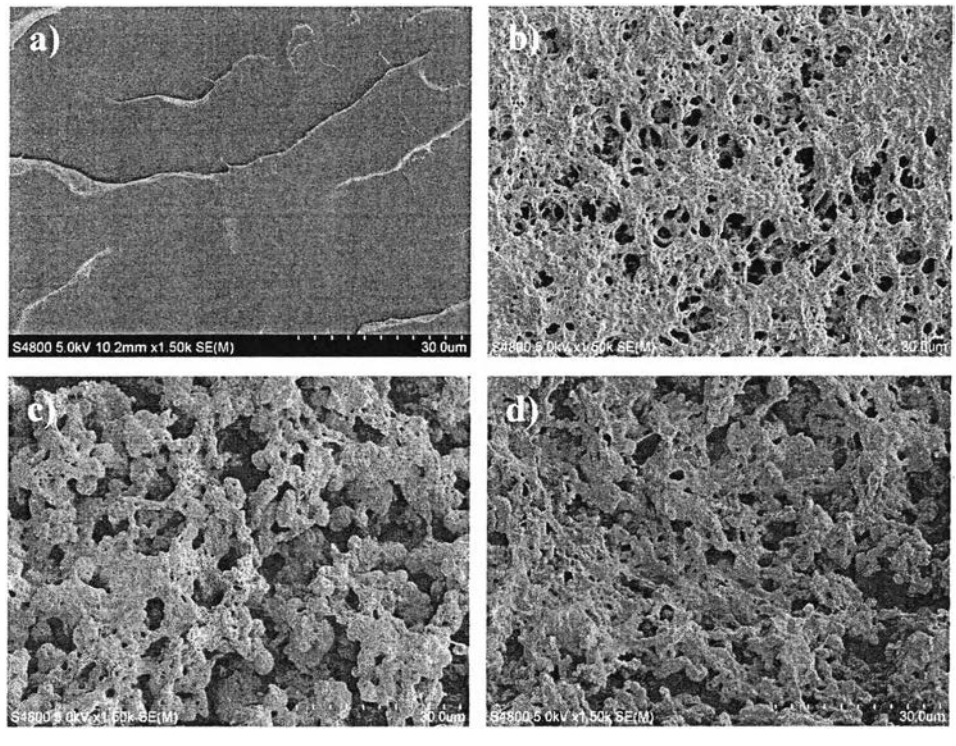

Figure 5.20. SEM image magnified at 1.5 k of copolymer a) pure PLA, b) ENR(5)-g-PLA(95) - 0.1 wt% $Sn(Oct)_2$, c) ENR(5)-g-PLA(95) - 0.2 wt% $Sn(Oct)_2$, and ENR(5)-g-PLA(95) - 0.3 wt% $Sn(Oct)_2$.

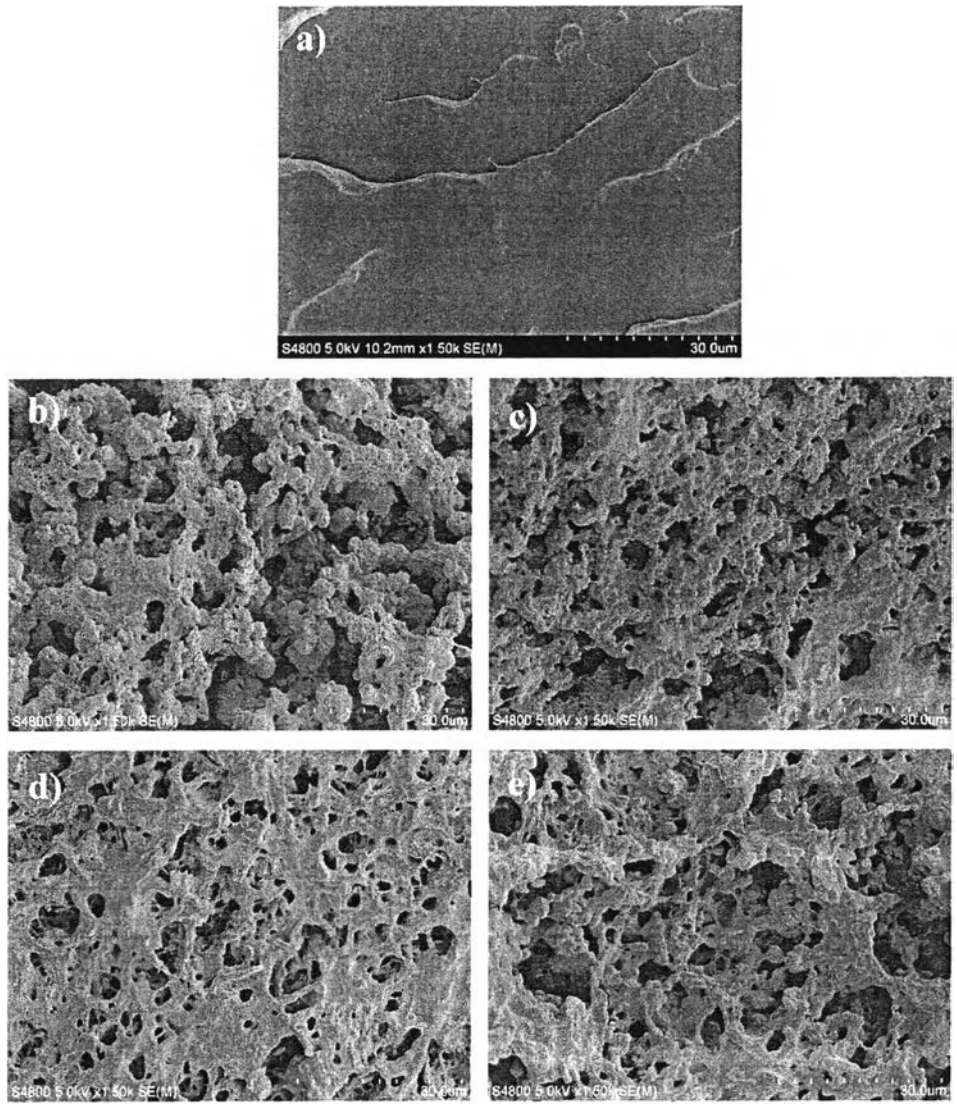

Figure 5.21. SEM micrograph magnified at 1.5 k of copolymer a) pure PLA, b) ENR(5)-g-PLA(95) - 0.2 wt% $Sn(Oct)_2$, c) ENR(10)-g-PLA(90) - 0.2 wt% $Sn(Oct)_2$, d) ENR(15)-g-PLA(85) - 0.2 wt% $Sn(Oct)_2$, and e) ENR(20)-g-PLA(80) - 0.2 wt% $Sn(Oct)_2$.

5.4.9 Biodegradable properties

The biodegradable properties are measured according to ASTM D5988 – 03. The percent weight loss of pure PLA and copolymers are shown in Figure 5.22 to 5.28. The weight loss values are illustrated in Table 5.8. The weight loss of sample decreases when compare with pure PLA. Moreover, the weight loss of copolymer decreases with increasing ENR content because the adding non-biodegradable polymer resulting in slowly degradation rate and ENR has more hydrocarbon part resulting in more hydrophobic part that effected to hardly degradation. However, the weight loss of copolymer increases with increasing catalyst concentration because the chain scission effect resulting in lower molecular weight and. The biodegradability is controlled by several factors such as the surface condition, the chemical structure, the molecular weight, the glass transition temperature, and the melting temperature [17].

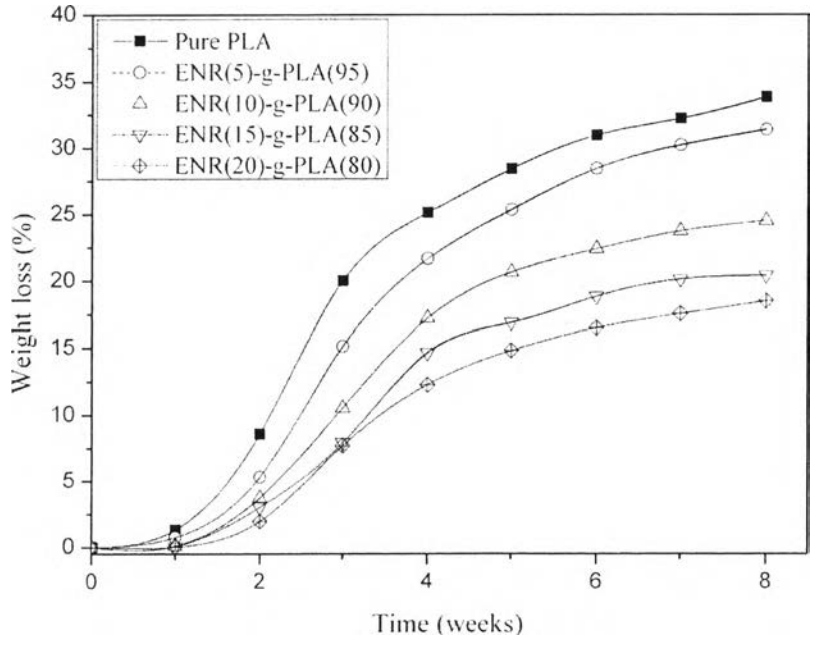

Figure 5.22. The percent weight loss of copolymer at 0.1 wt% $Sn(Oct)_2$ with different ENR contents.

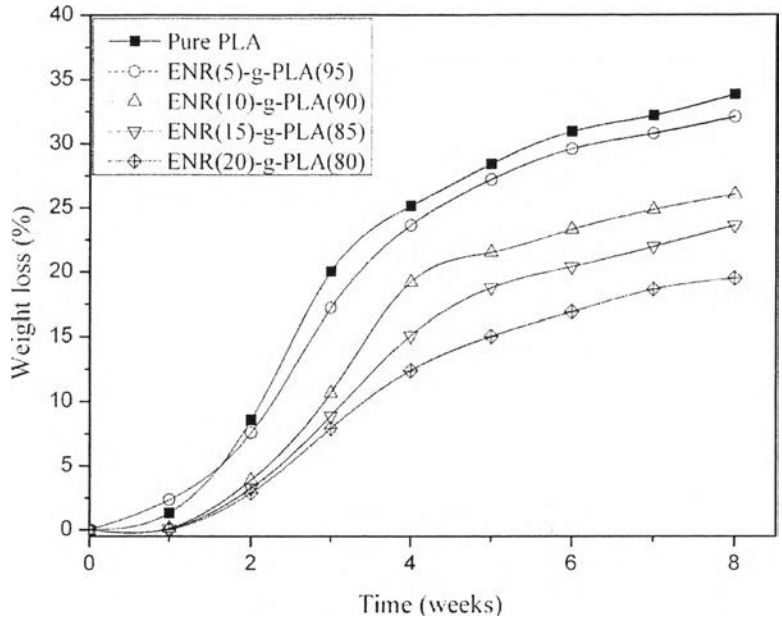

Figure 5.23. The percent weight loss of copolymer at 0.2 wt% $Sn(Oct)_2$ with different ENR contents.

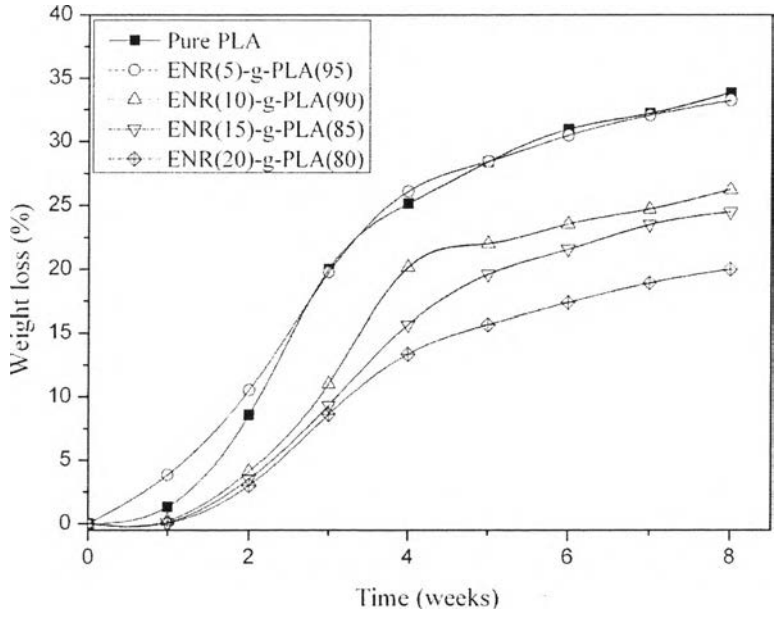

Figure 5.24. The percent weight loss of copolymer at 0.3 wt% $Sn(Oct)_2$ with different ENR contents.

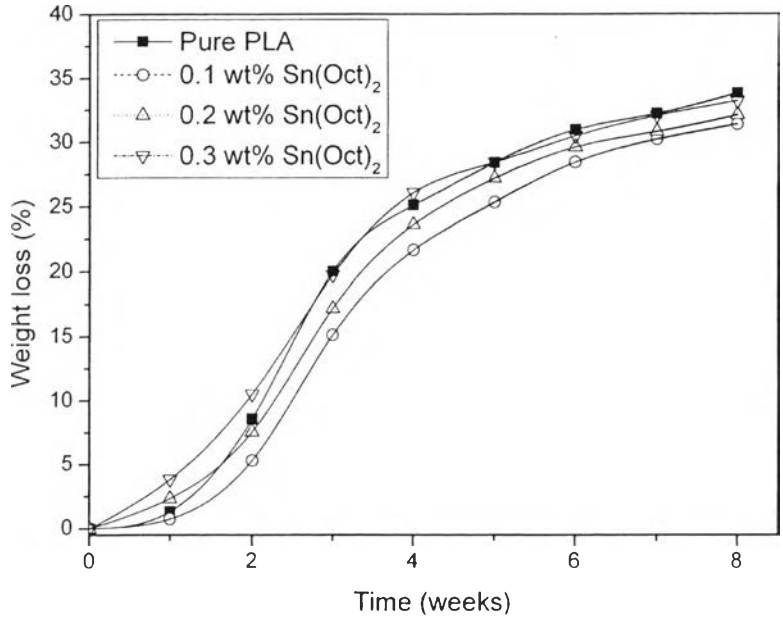

Figure 5.25. The percent weight loss of copolymer at 95/5 wt% of PLA/ENR with different catalyst concentrations.

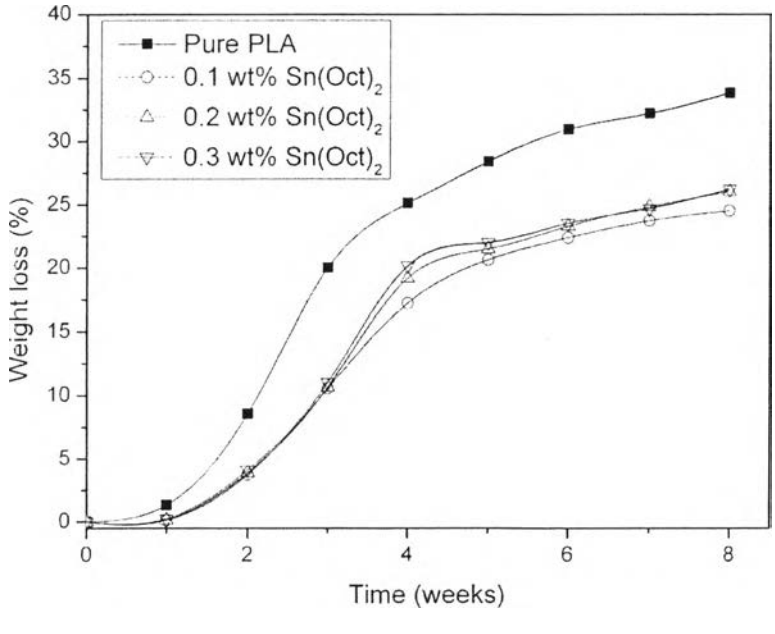

Figure 5.26. The percent weight loss of copolymer at 90/10 wt% of PLA/ENR with different catalyst concentrations.

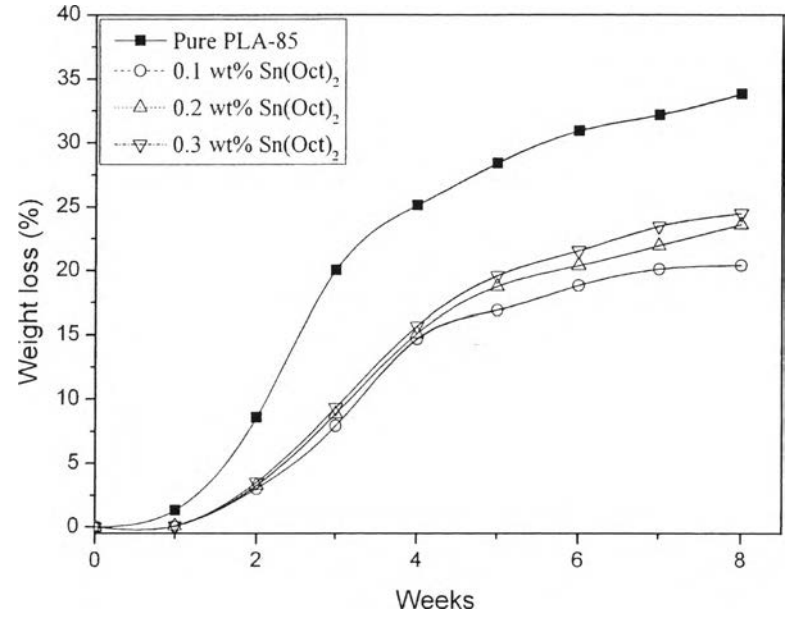

Figure 5.27. The percent weight loss of copolymer at 85/15 wt% of PLA/ENR with different catalyst concentrations.

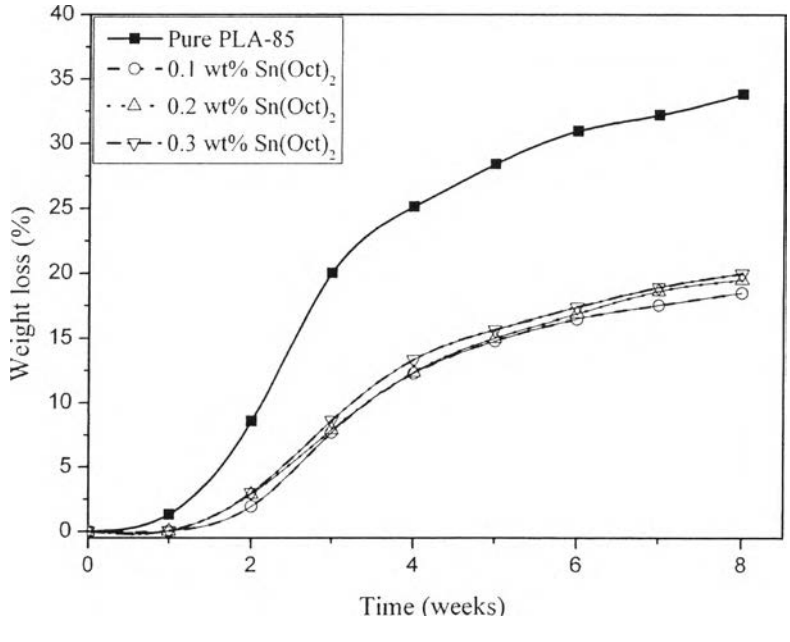

Figure 5.28. The percent weight loss of copolymer at 80/20 wt% of PLA/ENR with different catalyst concentrations.

5.4.10 Melt flow index (MFI)

The melt flow indexes of copolymer are measured by using Zwick, Model 4105 melt flow indexer. The Figure 5.29 and Table 5.9 show the MFI values of PLA and copolymer with various ENR content and catalyst concentration. The result clearly illustrate that the MFI decreases with ENR addition that corresponding to loss modulus as previously describe. Moreover, the viscosity of copolymer increase depends on reaction between ENR and PLA increase. The graft copolymer occurs at the side chain of copolymer resulting in the increasing of chain entanglement between molecules that effected to the viscosity increase. In addition, the viscosities of copolymer increase associate with the elastomeric behavior of ENR in copolymer [16]. In addition, the increasing of catalyst concentration that resulting in MFI increases because of chain scission effect [18].

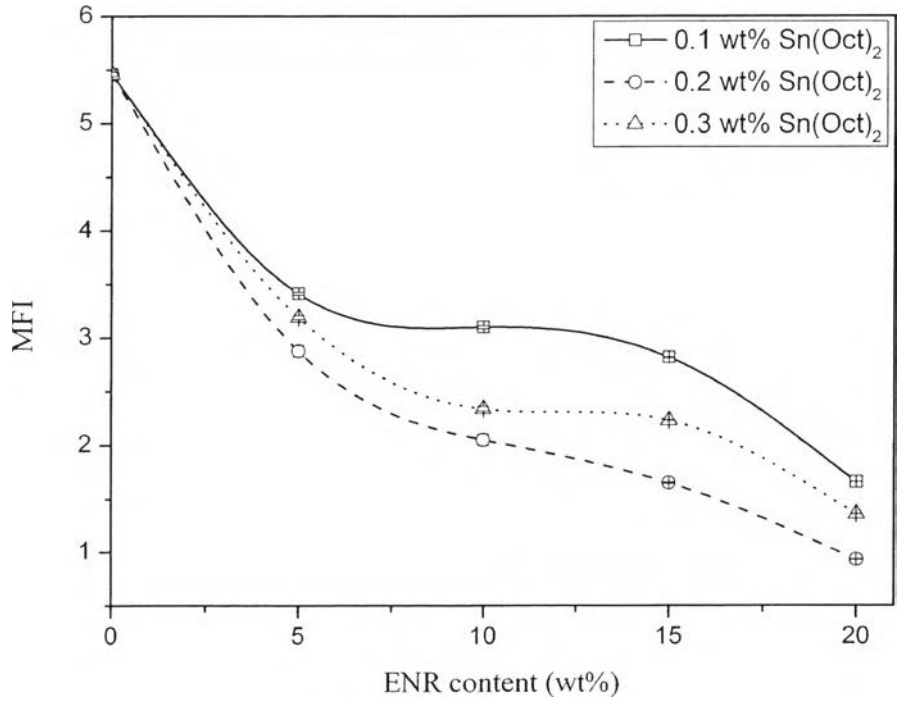

Figure 5.29. MFI of copolymer with various ENR content and catalyst.

Table 5.9 MFI value of copolymer

Sample (wt%)	Catalyst concentration (wt%)	MFI
ENR(5)-g-PLA(95)	0.1	3.41 ± 0.01
	0.2	2.88 ± 0.05
	0.3	3.19 ± 0.02
ENR(10)-g-PLA(90)	0.1	3.10 ± 0.02
	0.2	2.05 ± 0.05
	0.3	2.34 ± 0.02
ENR(15)-g-PLA(85)	0.1	2.92 ± 0.04
	0.2	1.25 ± 0.01
	0.3	2.43 ± 0.03
ENR(20)-g-PLA(80)	0.1	1.66 ± 0.01
	0.2	0.93 ± 0.01
	0.3	1.36 ± 0.01

5.5 Conclusion

The FTIR absorption spectrum confirms that copolymers of ENR-g-PLA are successfully prepared. The appearance peak at 1740 cm^{-1} (C=O group), 894 and 1655 cm^{-1} (C=C stretching), and 3400 cm^{-1} (-OH group) corresponding to ENR-g-PLA structure. The grafting percentage of ENR on PLA is around 24% with the ENR 20 wt%. Moreover, the DSC thermogram demonstrates that glass transition temperature and %crystallinity decrease because ENR obstructs the crystallization of PLA component. Furthermore, the thermo-mechanical results by DMA reveal that the introduction of ENR content improved flexibility of PLA chain observed by the decrease in storage modulus. For mechanical property, impact strength shows the greater value after adding ENR but their values are insignificantly different over various ENR content; however, the maximum ENR content is 15 wt%. The tensile test showed the Young's modulus is the same trend as the storage modulus from DMA. The elongation of copolymer was improved compared to pure PLA. Finally, the morphology of copolymer was investigated by FE-SEM which obviously revealed the well-dispersed ENR in PLA matrix.

5.6 Acknowledgement

This research is funded from The National Excellent Center for Petroleum, Petrochemicals, and Advanced Materials, Thailand, National Research Council of Thailand (NRCT), and Polymer Processing and Polymer Nanomaterial Research Units.

Finally, the author would like to give special thanks to advisors, Assoc. Prof. Rathanawan Magaraphan for her intensive suggestion, valuable guidance and vital help throughout this research. In addition, the author deeply thanks to Asst. Prof.Dr. Manit Nithitanakul and Assoc.Prof.Dr. Kalyanee Sirisinha for serving on her thesis committee.

5.7 Reference

1. Kricheldorf, H. (2001). Syntheses and application of polylactides. Chemosphere (43), 49-54.

2. Hyon,S.H., Jamshidi,K. and Ikada,Y. (1997). Synthesis of polylactides with different molecular weights. Biomaterials, *22* (18), 1503-1508.

3. Anderson, K.S. et al. (2008). Toughening Polylactide. Polymer Reviews, 1 (48), 85-108.

4. Gross, R.A. and Kalra, B. (2002). Biodegradable Polymers for the Environment. Science (297), 803-807.

5. Sterzel, H. (1995, June 6). Production of foamed polylactide injection moldings of high strength and rigidity. United State Patent .

6. Frick,E.M., Zalusky,A.S., and Hillmyer,M.A. (2003). Characterization of polylactide-b-polyisoprene-b-polylactide. Biomacromolecules (4), 216-223.

7. Nooeaid, P., M.S. Thesis, Chulalongkorn University, 2008.

8. Gelling, I. (1991). Epoxidised Natural Rubber. Journal of Natural Rubber Research . *3* (6), 184-205.

9. Nakason, C., Tobprakhon, A., Kaesaman A. (2005). Thermoplastic Vulcanizates Based on Poly(methyl methacrylate)/Epoxidized Natural Rubber Blends:Mechanical, Thermal, and Morphological Properties. Wiley InterScience , 1251-1261.

10. Liu, Y., Tian, F., and Hu, K.A. (2004). Synthesis and characterization of a brush-like copolymer of polylactide grafted onto chitosan. Carbohydrate Research, *339*, 845–851.

11. Zhang,C., Wang,W., Huang,Y., Pan,Y., Jiang,L., Dan,Y., Luo,Y., and Peng, Z. (2013). Thermal, mechanical and rheological properties of polylactide toughened by expoxidized natural rubber. Materials and Design (45), 198-205.

12. Chen,X., McCarthy,S.P., and Gross, R.A. (1997). Synthesis and characterization of [L]-lactide-ethylene oxide. Macromolecules (30), 4295-4301.

13. Nguyen,T.-H., Tangboriboonrat, P., Rattanasom, N., Petchsuk, A., and Opaprakasit, P. (2012). Journal Applied Polymer Science 124, 164-174.

14. Woo, Y., Jang, Y., Shin, T. J., Lee, R., and Narayan. (2007). Journal of Industrial and Engineering Chemistry 13(3), 457-464.

15. Ishida, S., Nagasaki, R., Chino, K., Dong, T., and Inoue, Y. (2009). Journal of Applied Polymer Science 113, 558-56.

16. Yew G.H. et al. (2005). Water absorption and enzymatic degradation of poly(lactic acid)/rice starch composites. Polymer Degradation and Stability (90), 488-500.

17. Tokiwa, Y., Calabia, B. P., Ugwu, C.U., and Aiba, S. (2009) Biodegradability of Plastics. International Journal of Molecular Sciences (10), 3722-3742.

18. Liu, Y. Y., Mohd Ishak, Z. A., Chow, W.S. (2012) Mechanical, Thermal, and Morphological Properties of Injection Molded Poly(lactic acid)/SEBS-g-MAH /Organo-Montmorillonite Nanocomposites. Journal of Applied Polymer Science, (124), 1200–1207.